ELSEVIER

Journal of Nuclear Materials 280 (2000) 295–303

journal of nuclear materials

www.elsevier.nl/locate/jnucmat

Lithium and tritium diffusion in lithium oxide (Li_2O), a molecular dynamics simulation

Heriberto Pfeiffer [a,*], Jorge Sánchez-Sánchez [b], Luis Javier Álvarez [b]

[a] *Departamento de Química, Universidad Autónoma Metropolitana-Iztapalapa, Av. Michoacán y la Purísima sln, Iztapalapa, C.P. 09340, México D.F., Mexico*

[b] *Laboratorio de Simulación de Materiales, Instituto de Matemáticas, Unidad Cuernavaca, Universidad Nacional Autónoma de México, Apdo. Postal 273-3, Admon 3., C.P. 62251 Cuernavaca, Morelos, Mexico*

Received 29 December 1999; accepted 14 April 2000

Abstract

Molecular dynamics simulations of Li_2O were performed in the microcanonical ensemble at several different temperatures in order to study the lithium diffusion process, and a preliminary exploration of the diffusion of tritium was performed. Different Li/O molar ratios were used to investigate the role of non-stoichiometry in the Li diffusion processes. The mechanism of lithium diffusion as a function of temperature is proposed based on the analysis of our simulations and a model is proposed to explain the overall behaviour of the lithium diffusion coefficient as a function of temperature. Our simulations suggest what is the role of hydrogen in the tritium release from breeder ceramic materials.

1. Introduction

There are a variety of breeder ceramic materials that could be employed in fusion reactors. All these materials have lithium as a common element. Lithium may be found as an isotope, ^{6}Li, in a concentration of 7.4 wt%. When this isotope is irradiated with thermal neutrons, the following fission reaction occurs [1]:

$$^6\mathrm{Li}(\mathrm{n},\alpha)^3\mathrm{H}, \quad E = 4.8\ \mathrm{MeV}. \tag{1}$$

In this reaction one tritium atom, ^{3}H, is formed and could be used as fuel in nuclear fusion reactors through a reaction between tritium and deuterium atoms producing 17.59 MeV per tritium atom, through [1,2]

$$^3\mathrm{H} +^2 \mathrm{H} \rightarrow^4 \mathrm{He} + \mathrm{n}. \tag{2}$$

Synthesis, characterisation, evaluation of radiation damages, and lithium and tritium diffusion have been studied in breeder ceramic materials considered for tritium production such as lithium oxide, lithium aluminates, silicates and zirconates [3–11]. Experimentally the diffusion coefficients vary between 5 and 6 orders of magnitude, and this is caused by a variety of factors such as host crystal size, morphology, purity of the sample, and temperature [12–16]. Tritium release is produced when the samples are purged with argon or helium, and further favoured when the gas is enriched with about 0.1% of hydrogen [10]. Even though all these studies represent a great effort to understand the mechanisms of diffusion of these important species, the exact mechanism by which tritium diffusion is activated and blocked as temperature rises in the interval 300–1200 K remains largely unknown. In sintered solid breeding materials, tritium release is composed of a series of migration steps and they still remain to be elucidated.

Simulation techniques may be very useful to elucidate the mechanism of tritium release [9]. However, some important characteristics of the system are to be determined before one is able to properly simulate the behaviour of tritium in the Li_2O lattice. As a first step towards this end we present in this paper molecular dynamics simulations of the Li_2O structure in order to study the role of non-stoichiometry in the temperature

* Corresponding author.
E-mail address: pfei@xanum.uam.mx (H. Pfeiffer).

0022-3115/00/$ - see front matter
PII: S0022-3115(00)00063-5

range 300–1200 K. This allows us to determine the probable composition of the real breeder material. As a preliminary exploration we introduced in the lattice a particle representing tritium, and show its possible behaviour.

2. Simulations

A good representation of the Li–O interaction for molecular dynamics purposes is a Pauling type interaction potential. This interaction law has been successfully used in a previous work on $LiAl_2O$ [9] and is given by

$$V(r_{ij}) = \frac{q_i q_j}{r_{ij}} + \frac{1}{n(\sigma_i + \sigma_j)} \left(\frac{\sigma_i + \sigma_j}{r_{ij}} \right)^n, \quad (3)$$

where q are the effective charges, and σ are the effective ionic radii. In a number of previous works we have chosen n to be equal to 9, since it has been determined to be the best value to represent partially ionic systems [19]. Effective radii are well determined quantities; therefore effective charges are the only parameters to be determined in order to represent the interactions Li–Li, Li–O, and O–O. We fitted the charges in such a way as to obtain the heat of formation, ΔH^0, of $Li_2O_{0.96}$ arranged in a cubic box with periodic boundary conditions, according to the structure reported by De Vita, et al. [20], obtaining −598.1 kJ/mol whereas the experimental ΔH^0 is equal to −596.1 kJ/mol [21]. This system consisted of 758 particles of which 512 particles correspond to lithium atoms and 246 particles to oxygen atoms, assuming that the system would loose oxygen upon heating. In previous works we have studied the role of non-stoichiometry in crystals. Realistic interaction potentials cannot be obtained if perfect crystals are considered to fit the interaction potential parameters since the melting point of perfect crystals, which do not occur in nature, is overestimated in molecular dynamics simulations [17,18]. As we mentioned in the previous section, one first step in the simulation studies of Li_2O is to determine the probable composition of the real breeder material. Therefore, as we shall see in what follows, we considered three different systems with different stoichiometries: $Li_2O_{0.96}$, Li_2O, and $Li_{1.9}O$ for which the radii and charges are shown in Table 1. The charges of the non-stoichiometric systems were determined fixing the charge of lithium and changing the charge of oxygen accordingly in order to obtain an electroneutral system. This was done based on the assumption that upon removal of either oxygen or lithium the resulting extra charge would spread over oxygen atoms.

In order to test the interaction potential we determined the simulated melting point exploring the behaviour of ΔH^0 vs temperature of $Li_2O_{0.96}$. Fig. 1 shows this plot where there is a clear discontinuity of the straight line between 1660 and 1715 K, which means that at this point there is a phase transition. In this case, the transition corresponds to the melting point of the non-stoichiometric system, which we estimate to be at 1687 K in excellent agreement with the experimental melting point of 1700 K.

Table 1
Interaction potential parameters

System	Lithium		Oxygen	
	σ (nm)	q (e)	σ (nm)	q (e)
$Li_2O_{0.96}$	0.073	0.86	0.124	−1.789
Li_2O	0.073	0.86	0.124	−1.720
$Li_{1.9}O$	0.073	0.86	0.124	−1.634

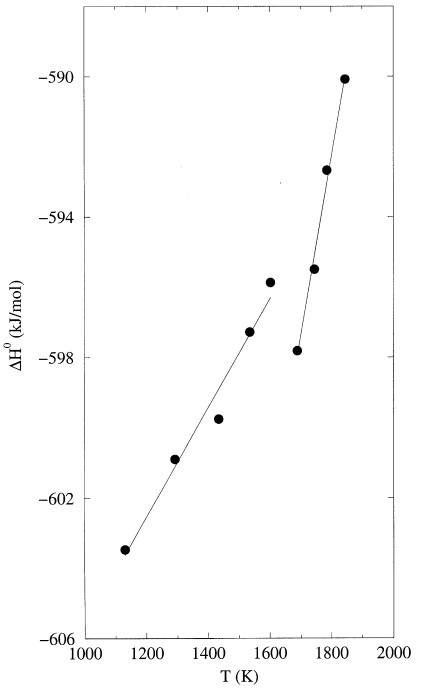

Fig. 1. Variation of the heat of formation, ΔH^0, as a function of temperature for the $Li_2O_{0.96}$ system.

The real composition of lithium oxide in breeding experiments at high temperature has not been determined experimentally, although it is to be expected that the system would be non-stoichiometric as a consequence of heating and thermal neutron irradiation. Therefore, in order to perform realistic simulations this composition had to be approximately determined based on known properties of the system, which would depend on the type of deficiencies leading to non-stoichiometry. Tritium release is known to be enhanced in the temperature interval 500–700 K and it has been suggested that it is intimately associated to lithium diffusion [8].

Therefore the system we chose to study is that which presents diffusion of lithium in the same temperature range as the experimentally tritium release enhancement. To determine the composition that leads to non-stoichiometry we set up three different systems: First, the perfect crystal; second, a system with a lithium deficiency of 2 wt%; and third, a system with an oxygen deficiency also of 2 wt%. The first system was constituted by 768 particles, 512 represented lithium atoms and 256 oxygen atoms with a Li/O ratio of 2. The second system consisted of 758 particles of which 512 represented lithium atoms and 246 oxygen atoms in a crystalline structure with a Li/O ratio of 2.083 corresponding to a non-stoichiometric compound $Li_2O_{0.96}$, obtained by randomly removing 10 oxygen atoms from the original perfect system. The third system was constituted by 743 particles of which 487 represent lithium atoms and 256 oxygen atoms with a Li/O ratio of 1.90 corresponding to $Li_{1.9}O$. In this case 25 lithium atoms were randomly removed from the original system.

Simulations were performed at temperatures of 300, 600, 900 and 1200 K. At the beginning of every calculation a thermalisation run was performed rescaling the velocities of all particles every time step for 5 ps. Then a run of 2.5 ps without temperature control in order to relax the system to ensure thermodynamic equilibrium. Finally a run of 7.5 ps in which accumulation of the relevant quantities was carried out to calculate the final statistical averages. The integration of the classical equations of motion was carried out using standard techniques and long range forces were calculated with the Ewald summation method [22].

3. Results and discussion

3.1. Structure

The structural behaviour of the three 'samples' studied upon heating, Li_2O, $Li_2O_{0.96}$, and $Li_{1.9}O$, was analysed and the result is that the sample with a Li/O ratio of 1.9 is the one that better represents the real system. Fig. 2 shows the partial radial distribution functions, $g(r_{Li-Li})$, $g(r_{Li-O})$ and $g(r_{O-O})$, of the final

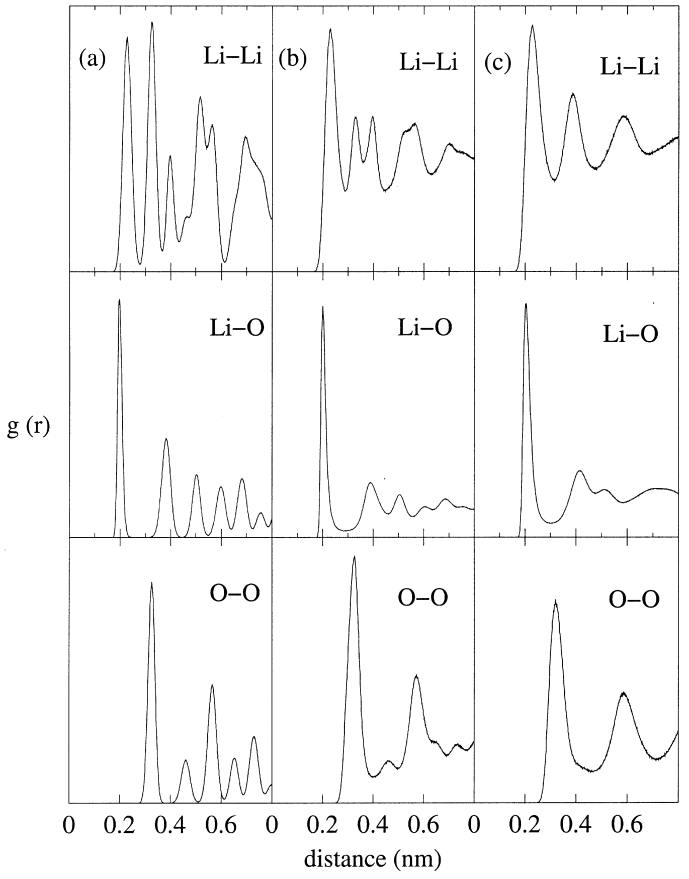

Fig. 2. Partial radial distribution functions, at 1200 K for the three different systems: (a) Li_2O; (b) $Li_{1.90}O$; (c) $Li_2O_{0.96}$.

structures of the three different systems at 1200 K. As it can be seen, $Li_{1.9}O$ preserves the overall crystalline structure whereas $Li_2O_{0.96}$ losses the long range order. The real system at this temperature is partially crystalline, even though the structure is damaged by thermal treatment and by the exposure to thermal neutron radiation. Since the temperature at which we report the $g(r)$ is around 500 degrees below the melting point it is evident that $Li_{1.9}O$ has a behaviour closer to that of the real system than the simulated $Li_2O_{0.96}$. This is reflected in that both short and long range order are essentially preserved in the simulated damaged structure.

Fig. 3 shows snapshots of the final configurations of the three samples after the run at 1200 K. Fig. 3(a) and (b) shows the ideal crystalline configuration and the simulated ideal crystal (Li_2O), respectively. The few differences between these configurations are due to small displacements of atoms and to the effect obtained by imposing periodic boundary conditions in the molecular dynamics simulations; however, it is clear from these figures that the structure remains unchanged. Fig. 3(c) corresponds to the disordered structure of $Li_2O_{0.96}$ whereas Fig. 3(d) is the one corresponding to $Li_{1.9}O$. In the latter the order is obviously preserved and lithium vacancies are hardly appreciated. A lithium vacancy is indicated by an arrow in the corresponding figure. The effect of having a Li vacancy is the generation of a local dislocation of the neighbouring Li atoms, with the concomitant displacement of the oxygen atoms in their vicinity. This effect produces lengthening of the Li–O and O–O bond distances as can be seen from Table 2

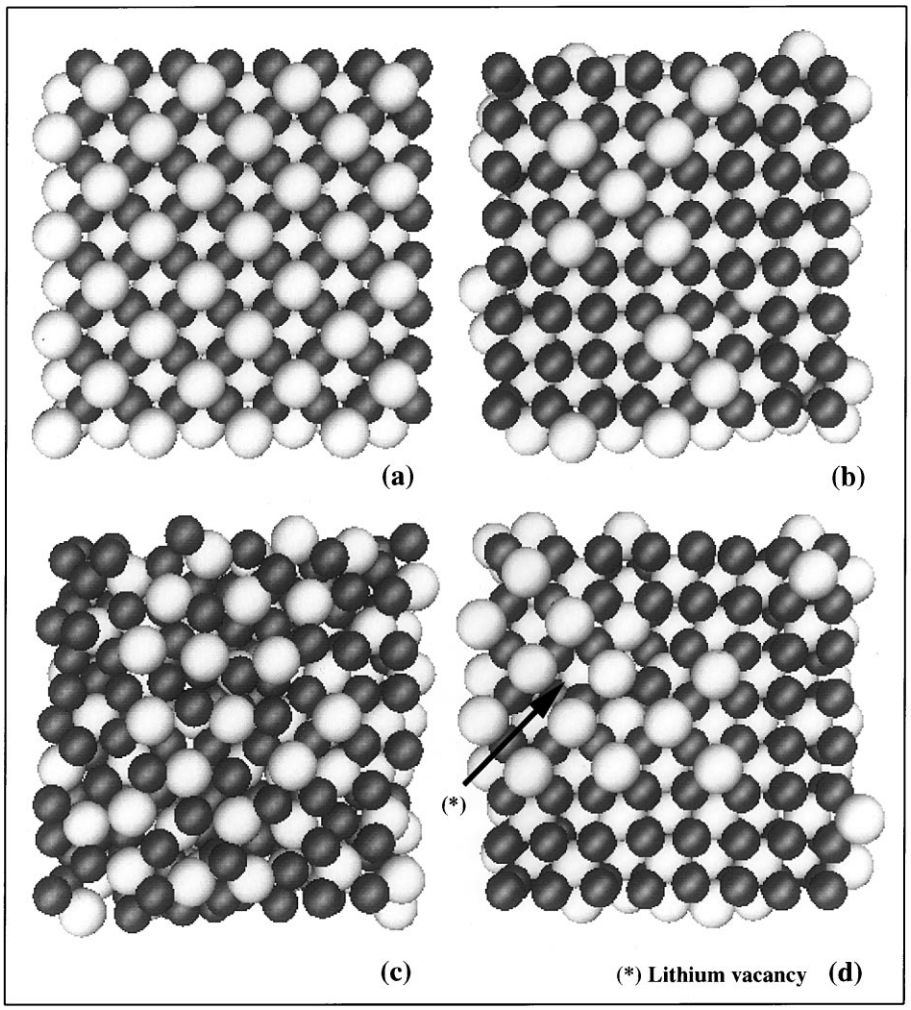

Fig. 3. Snapshots of the final configurations for the different systems, at 1200 K: (a) initial configuration; (b) Li_2O; (c) $Li_2O_{0.96}$; (d) $Li_{1.90}O$. In the snapshots the bigger and highlighted spheres correspond to oxygen atoms, and the dark and smaller spheres correspond to lithium atoms.

Table 2
Positions of the first three peaks of the partial radial distribution functions for the three systems studied

$g(r)$	Li_2O (nm)	$Li_2O_{1.96}$ (nm)	$Li_{1.9}O$ (nm)
Li–O	0.198	0.206	0.206
O–O	0.329	0.314	0.332
Li–Li	0.232	0.236	0.232

were the positions of the first three peaks of the partial radial distribution functions are shown.

3.2. Diffusion

Einstein relation between the mean square displacement as a function of time, $m(t)$, and the self-diffusion coefficient allows for the calculation of the diffusion coefficient, D, of any species in the system through

$$2tD = \frac{1}{3}\left\langle |r_i(t) - r_i(0)|^2 \right\rangle, \tag{4}$$

where r is the position of the diffusing species, t the time, and the brackets indicate a time average. This relation indicates that a diffusion process is occurring when the slope of the long time tail of the mean square displacement, $m(t)$, is different from zero.

Fig. 4 shows the mean square displacement of all species for the three different systems at 300, 600, 900 and 1200 K. For the perfect crystal, there is no diffusion of any species at any temperature, due to the lack of mobility of species imposed by the lack of vacancies.

$Li_2O_{0.96}$ presents no diffusion at all of oxygen atoms at $T = 300$, and 600 K. At 900 K there is very little motion of Li atoms. At 1200 K there is a change in the slope of the $m(t)$ vs t plot at around 5 ps of

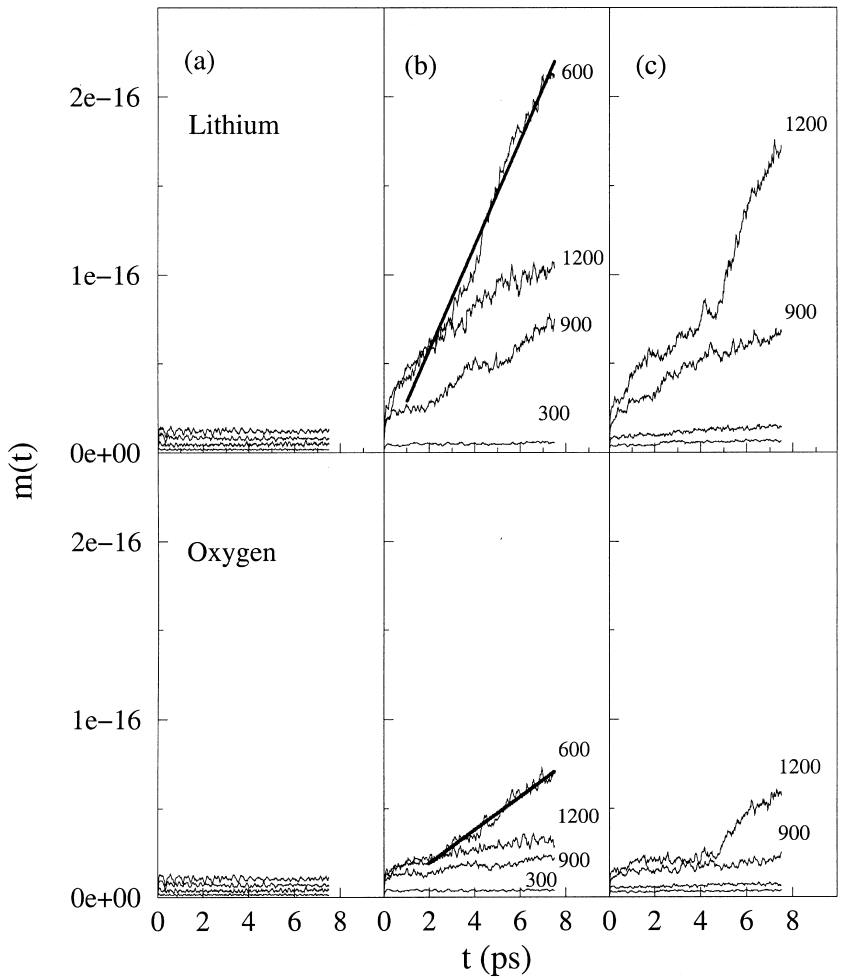

Fig. 4. Mean square displacement plots for the different species in the three different systems, at 300, 600, 900 and 1200 K: (a) Li_2O; (b) $Li_{1.90}O$; (c) $Li_2O_{0.96}$.

simulated time for both Li and O, indicating a generalised motion of atoms. This result is in agreement with the experimental fact that heating the sample in an oxygen free atmosphere may lead to a structural phase transition that, in turn, eventually leads to the melting of the system. This has been observed in other oxides with a much higher melting point, such as Y_2O_3 [17,23].

The results of $Li_{1.9}O$ are very clear. At temperatures of 300, 900 and 1200 K the self-diffusion coefficient of both species are very low compared to the one at 600 K, as it can be seen from the $m(t)$ vs t plots. Note that the self-diffusion coefficient of lithium, proportional to the slope of the straight line in the upper central panel of Fig. 4, is about three times that of oxygen, and it is due to steric repulsion (lower central panel). This result is in agreement with the experimental observation that tritium release is enhanced in the interval 500–700 K. On the other hand, it confirms that tritium may lag lithium in the diffusion process [20], being lithium considerably more mobile than oxygen. As we shall show in what follows, lithium mobility is higher than tritium mobility, as well.

These results become very clear in Fig. 5 in which we have plotted the diffusion coefficients, D, of Li and O for the two non-stoichiometric systems as a function of temperature. In the case of $Li_{1.9}O$ both species show a D maximum at 600 K, whereas $Li_2O_{0.96}$ have an increasing tendency with increasing temperature. Based on these results and considerations our first conclusion is that the real system has probably an important lack of lithium atoms, although the lack of oxygen atoms is not precluded. In any case our results strongly suggest that the real system is non-stoichiometric. From this point on, we will be referring only to the $Li_{1.9}O$ system.

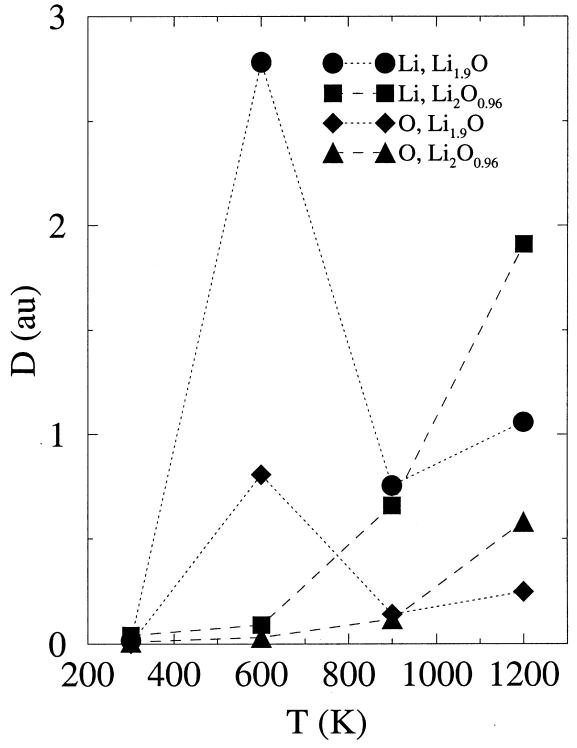

Fig. 5. Self-diffusion coefficients of lithium and oxygen in $Li_{1.90}O$ and $Li_2O_{0.96}$ simulated systems as a function of temperature.

In order to understand the diffusion mechanism as a function of temperature, a detailed coordination analysis of all atoms was performed. Molecular dynamics simulations allow for this sort of coordination number analysis. The average coordination numbers of lithium atoms at 300 and 600 K are 4.05 and 4.14, respectively, as can be seen from Fig. 6, where we have plotted the percentage of Li and O atoms against coordination number. These values are in good agreement with experimental estimations that report a value of four [20]. The average coordination number of lithium increases to 4.86 and 4.83 when temperatures are raised to 900 and 1200 K, respectively. Average oxygen coordination numbers go from 8 to 9 when temperature increases beyond 600 K.

The results of the calculation of the mean square displacement and coordination numbers for different temperatures, along with the fact that the original structure has a number of tetrahedral Schottky defects, strongly suggest that four coordinated lithium atoms are preferentially diffusing by hopping from one tetrahedral vacancy to another. The activation energy of the Li diffusion mechanism is reached only at around 600 K. Therefore there is no diffusion at temperatures lower than this limit. Beyond 600 K the diffusion coefficient is lower than that at 600 K due to the onset of a structural transformation of the system, indicated by the increase of the average coordination number, which inhibits diffusion by increasing bond energy of both species. The populations of four coordinated lithium are 465 and 436 at 300 and 600 K, respectively, whereas at 900 and 1200 K are 131 and 153, respectively. On the other hand the population of five coordinated lithium atoms at 300 and 600 K are 15 and 33, as opposed to 283 and 256 at 900 and 1200 K, respectively (see Table 3). Diffusion of lithium is enhanced at 600 K because tetrahedral vacancies are still available in the structure and the activation energy of the process has already been reached. Fig. 7 shows the partial radial distribution function for the Li–O pair for the four simulated temperatures. At 600 K there still is some long range order, whereas at 900 and 1200 K there is only short range order. This confirms the statement that an order-disorder structural transformation of the system starts beyond 600 K.

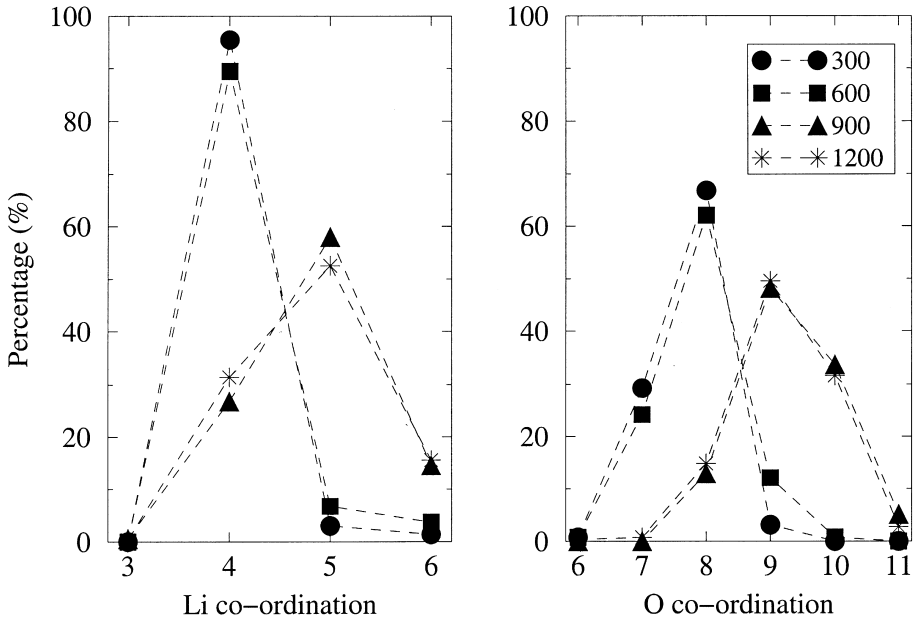

Fig. 6. Lithium and oxygen coordination numbers, at the different temperatures, for the $Li_{1.90}O$ system.

Table 3
Coordination number populations for Li in $Li_{1.90}O$ as a function of temperature

Coordination number	Temperature (K)			
	300	600	900	1200
3	–	–	3	2
4	465	436	131	153
5	15	33	283	256
6	7	18	70	76
Average	4.05	4.14	4.86	4.83

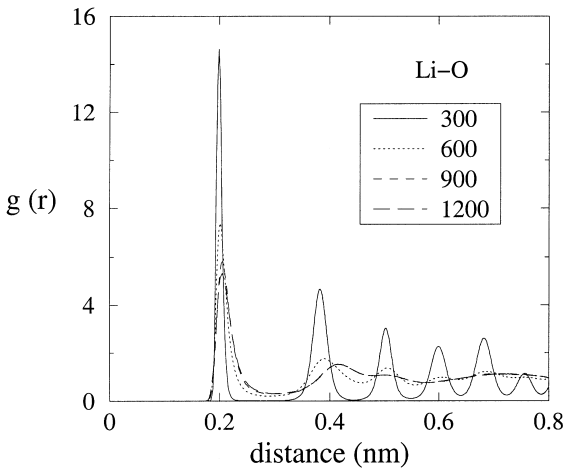

Fig. 7. Partial radial distribution functions, for the Li–O bond in the $Li_{1.90}O$ system, at four different temperatures.

3.3. Tritium diffusion

In order to study tritium behaviour within lithium oxide we introduced a particle with a mass of 3.006 atomic mass units, a charge of 1*e*, and a radius of 0.048 nm in a location determined at random in the $Li_{1.90}O$ system. Fig. 8 shows the $m(t)$ vs t for the three species present in the system. Lithium and oxygen atoms present the same behaviour as in the pure lithium oxide system. in the sense that they have a maximum at 600 K. However the relative value of the diffusion coefficient of Li is around 30% lower than in the system without tritium. Something similar happens for oxygen atoms. Tritium atom quickly diffuses at very short times of around 0.1 ps at all temperatures. After this short time, the slope of the $m(t)$ vs t, is equal to zero for the systems at 300 to 900 K, indicating that tritium atom does not diffuse. At 1200 K the plot shows a different behaviour. Apparently the tritium atom diffused quickly in the first 2 ps, but at the end of the 7.5 ps it returns nearly to its initial position. Therefore the lowering of the diffusion coefficient for both Li and O may clearly be ascribed to the trapping of tritium. Fig. 9 shows a snapshot of the local configuration around the tritium atom at the end of the run. It is centred in a tetrahedron and is surrounded by oxygen atoms located in the corners of the tetrahedron. Evidently tritium is located in an already existing lithium vacancy preserving the bond distances of about 0.2 nm at all temperatures. The fact that tritium is trapped in a tetrahedral cavity suggests the reason why the inert gas flux used to drag out tritium from the

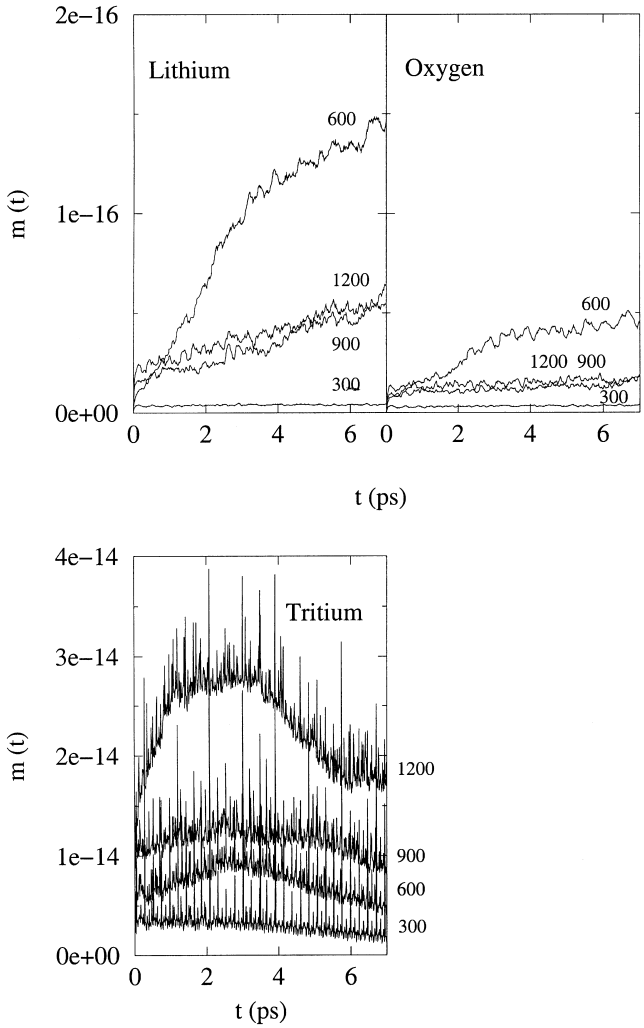

Fig. 8. Mean square displacement plots for the different species in the $Li_{1.90}O$ system with one tritium atom placed in a random position, at 300, 600, 900 and 1200 K.

ceramic material has to be enriched with hydrogen in order to enhance tritium release. The presence of hydrogen in the network would weaken T–O bonds favouring the release of tritium and lowering the activation energy of tritium diffusion processes. The role of hydrogen is expected to be very similar in all breeder ceramic materials.

Apparently, the fact that tritium does not diffuse in the same conditions in which lithium diffuses, is due to the extra charge, which amounts to 30% more than that of lithium. Tritium charge is large enough to hold it in the tetrahedral cavity. Experimentally tritium release is achieved by introducing an inert gas flux enriched with hydrogen. The inert gas flux would impinge kinetic energy to tritium, and the high reactivity of hydrogen would decrease the bond energy of tritium in the cavity, upon the formation of OH species. These two effects combined facilitate the release of tritium from breeder ceramic materials.

4. Conclusions

We have performed molecular dynamics simulations of lithium oxide with different Li/O molar ratios in order to find out what is the role of non-stoichiometry in the process of lithium and possibly tritium diffusion. This was suggested by the experimental evidence that the best conditions for the tritium release are in the temperature range 500–700 K and a purge gas of argon or helium containing 0.1% of hydrogen. Our simulations indicate that when no oxygen or lithium vacancies are generated

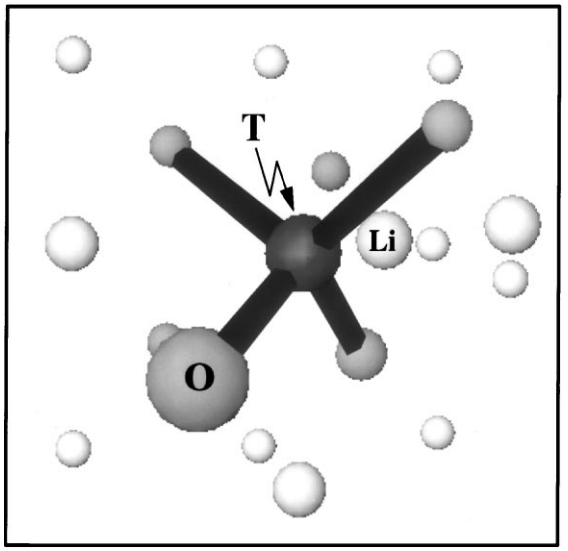

Fig. 9. Location of tritium in the final structure of $Li_{1.90}O$ at 1200 K.

there is not diffusion of any species. When the crystal losses oxygen atoms the crystal structure rapidly changes to an amorphous structure. The non-stoichiometric system $Li_{1.9}O$ does not undergo phase transitions at high temperatures and allows for lithium diffusion, behaving in a very similar fashion as the real system. Our simulations show that the best temperature for diffusion of lithium atoms is 600 K, in agreement with experimental observations. Based on our simulations we propose an explanation of the overall behaviour of the lithium diffusion coefficient as a function of temperature.

Acknowledgements

H.F. thanks Consejo Nacional de Ciencia y Tecnología (CONACyT) México for financial support during the development of this work. Thanks are due to an anonymous reviewer for suggestions for improvement of the paper.

References

[1] M. Nagai, M. Hibino, T. Nishino, K. Noda, J. Mater. Sci. Lett. 12 (1993) 107.
[2] R.L. Murray, Nuclear Energy: Introduction to the Concepts, Systems and Applications of Nuclear Processes, 3rd Ed., Pergamon, Canada, 1988.
[3] H. Pfeiffer, P. Bosch, S. Bulbulian, J. Nucl. Mater. 257 (1998) 309.
[4] C.E. Johnson, K.R. Kummerer, E. Roth, J. Nucl. Mater. 155–157 (1988) 188.
[5] D. Vollath, H. Wedemeyer, E. Günter, J. Nucl. Mater. 133&134 (1985) 221.
[6] M. Smaihi, J.P. Boilot, F. Botter, J. Mougin, M.J. Boncoeur, J. Nucl. Mater. 185 (1991) 19.
[7] F. Beuneu, P. Vajda, Phys. Rev. Lett. 76 (1996) 4544.
[8] J.P. Kopasz, C.A. Seils, C.E. Johnson, J. Nucl. Mater. 212–215 (1994) 912.
[9] J.P. Jacobs, M.A. San-Miguel, L.J. Álvarez, P. Bosch, J. Nucl. Mater. 232 (1996) 131.
[10] C.E. Johnson, J.P. Kopasz, S.W. Tam, J. Nucl. Mater. 248 (1997) 91.
[11] S. Tanaka, M. Taniguchi, J. Nucl. Mater. 248 (1997) 101.
[12] B. Rasneur, Adv. Ceram. 27 (1990) 63.
[13] K. Noda, Y. Ishii, H. Ohno, H. Watanabe, Adv. Ceram. 27 (1990) 173.
[14] H. Ohno, S. Konishi, T. Nagasaki, T. Kurasawa, H. Katsuta, H. Watanabe, J. Nucl. Mater. 133&134 (1985) 181.
[15] J.P. Kopasz, S.W. Tam, C.E. Johnson, J. Nucl. Mater. 155–157 (1988) 500.
[16] D. Yamaki, S. Tanaka, M. Yamawki, J. Nucl. Mater. 212–215 (1994) 917.
[17] L.J. Álvarez, M.A. San-Miguel, J.A. Odriozola, Phys. Rev. B 59 (1999) 11303.
[18] M.A. SanMiguel, L.J. Álvarez, J. Fernández-Sanz, J.A. Odriozola, J. Molec. Struc. 463 (1999) 185.
[19] D.J. Adams, I.R. McDonald, Physica B 79 (1975) 159.
[20] A. DeVita, M.J. Gillan, J.S. Lin, M.C. Payne, I. Stich, L.J. Clarke, Phys. Rev. Lett. 68 (1992) 3319.
[21] R.C. Weast, M.J. Astle (Eds.), CRC Handbook of Chemistry and Physics, 63rd Ed., CRC, Boca Raton, FL, 1982.
[22] M.P. Allen, D.J. Tildesley, Computer Simulation of Liquids, Clarendon, Oxford, 1987.
[23] S. Krishnan, S. Ansell, D.L. Price, J. Am. Ceram. Soc. 81 (1998) 1967.